Rebuilding the Injured Brain: Use of MRS in Clinical Regenerative Medicine

Alina Zare[1], Michael Weiss[2], Paul Gader[3]
[1]Electrical and Computer Engineering, University of Missouri, Columbia, MO 65211
[2]McKnight Brain Institute, Department of Pediatrics, University of Florida, Gainesville, FL 32611
[3]Computer and Information Science and Engineering, University of Florida, Gainesville, FL 32611

ABSTRACT

Hypoxic-Ischemic Encephalopathy (HIE) is the brain manifestation of systemic asphyxia that occurs in 20 out of 1000 births. HIE triggers an immediate neuronal and glial injury leading to necrosis secondary to cellular edema and lysis. Because of this destructive neuronal injury, up to 25% of neonates exhibit severe permanent neuropsychological handicaps in the form of cerebral palsy, with or without associated mental retardation, learning disabilities, or epilepsy. Due to the devastating consequences of HIE, much research has focused on interrupting the cascade of events triggered by HIE. To date, none of these therapies, with the exception of hypothermia, have been successful in the clinical environment. Even in the case of hypothermia, only neonates with mild to moderate HIE respond to therapy. Stem cell therapy offers an attractive potential treatment for HIE. The ability to replace necrotic cells with functional cells could limit the degree of long-term neurological deficits. The neonatal brain offers a unique milieu for stem cell therapy due to its overall plasticity and the continued division of cells in the sub-ventricular zones.

New powerful imaging tools allow researchers to track stem cells *in vivo* post-transplant, as shown in Figure 1. However, neuroimaging still leaves numerous questions unresolved: How can we identify stem cells without using tracking agents, what cells types are destroyed in the brain post injury? What is the final phenotypic fate of transplanted cells? Are the transplanted cells still viable? Do the transplanted cells spare endogenous neuronal tissue? We hypothesize that magnetic resonance spectroscopy (MRS), a broadly used clinical technique that can be performed at the time of a standard MRI scan, can provide answers to these questions when coupled with advanced computational approaches. MRS is widely available clinically, and is a relative measure of different metabolites within the sampled area. These measures are presented as a series of peaks at a particular bandwidth that corresponds to an individual metabolite, such as lactate or creatine, as shown in Figure 2. Currently, the data are only subjectively interpreted by a neuro-radiologist, but hold great potential if they were analyzed in a more objective manner.

The overall purpose of the research described here is to develop pattern recognition algorithms for MRS data as a means to detect novel biomarkers or fingerprints of stem cells. Once identified, this technique will be used to identify *in vivo* transplanted stem cells within the brain.

Keywords: Regenerative Medicine, Magnetic Resonance Spectroscopy, Spectral Unmixing

1. METHODS

The goal of this work is to investigate the potential of using advanced pattern recognition techniques to objectively analyze data collected using MRS. The various peaks within a MRS spectrum can used to identify individual metabolites. The combination of these metabolite peaks may be then used to identify particular cell types. The pattern recognition techniques employed stem from the hyperspectral data analysis literature for spectral unmixing[18, 23, 24, 25]. Spectral unmixing approaches are used to decompose a spectrum into its respective *endmembers* and *proportions*. The endmembers are the spectral signatures which correspond to the constituent materials. In the work shown here, the endmembers correspond to the spectral signatures, or the fingerprints, containing the collection of metabolite peaks corresponding to each cell type. The proportions indicate the percentage of a spectrum which is associated with each endmember. For example, a sample over which an MRS spectrum is collected that contains an even amount of two cell types would have proportion values of 0.5 for each cell type.

Several endmember detection and spectral unmixing algorithms are described in the hyperspectral unmixing literature. These algorithms are often a combination of both endmember detection and spectral unmixing. Therefore, in

Medical Imaging 2011: Biomedical Applications in Molecular, Structural, and Functional Imaging,
edited by John B. Weaver, Robert C. Molthen, Proc. of SPIE Vol. 7965, 796516 · ©
2011 SPIE · CCC code: 0277-786X/11/$18 · doi: 10.1117/12.877805

these methods, the spectral signature for each endmember is estimated as well as the proportion of each endmember found in every spectral sample under consideration. Many of these methods assume that a pure spectral signature can be found in a data set. (i.e. There is a sample in a data set for each cell type that contains a spectral response only from that endmember.)[26, 27, 28] There have also been methods based on Non-negative Matrix Factorization[30, 31, 32, 33], Independent Components Analysis[24, 35], and others[36, 37, 38, 39]. Recent studies have also included methods which search for multiple sets of endmembers and endmember distributions[17]. The hyperspectral unmixing algorithms generally rely on the Convex Geometry Model (or the Linear Mixing Model). The convex geometry model assumes that each spectrum is a convex combination of the endmember spectra.

For this investigation, data were collected using MRS as described in Section 2. Given samples with varying amounts of different cell types, the proposed pattern recognition algorithm estimates the proportion of each cell type in a sample using spectral unmixing techniques based on the convex geometry model[17, 18]. The proportions estimated using the spectral unmixing techniques are compared with the amounts of each cell type estimated by a human expert for each sample.

The convex geometry model states that each spectrum (i.e., an MRS spectrum) is a convex combination of the endmember spectra. In the data collected for this study, the endmembers correspond to the spectral signatures of samples containing only a single cell type. The convex geometry model can be written as shown in Equation 1.

$$\mathbf{X}_i = \sum_{k=1}^{M} p_{ik}\mathbf{E}_k + \varepsilon_i \qquad i = 1,\ldots, N \tag{1}$$

where N is the number of measured spectra, M is the number of endmembers, ε_i is an error term, p_{ik} is the proportion of endmember k in spectrum i, and $\mathbf{E}_k$ is the k^{th} endmember. In this model, the proportions satisfy the following constraints.

$$p_{ik} \geq 0, k = 1,\ldots M, \qquad \sum_{k=1}^{M} p_{ik} = 1. \tag{2}$$

Using this model, the proportions of each cell type can be estimated given the spectral signatures of the endmembers. In the research presented here, the endmembers were measured using MRS and their spectral signatures were used in conjunction with the convex geometry model to solve for the proportions of each cell type in every MRS spectrum measured. The proportions are estimated using a quadratic programming step by minimizing the squared error of the MRS spectra and its estimate using endmembers and proportions subject to the constrains shown in Equation 2.

$$RSS = \sum_{i=1}^{N}\left(\mathbf{X}_i - \sum_{k=1}^{M} p_{ik}\mathbf{E}_k\right)^T\left(\mathbf{X}_i - \sum_{k=1}^{M} p_{ik}\mathbf{E}_k\right) \tag{3}$$

Therefore, given the endmember spectral signatures collected over samples from containing only a single cell type, the proportions for each sample collected over a mixture of cell types was estimated by solving for the proportions using a quadratic programming step which minimizes the objective function in Equation 3. Since the proportions associated with each MRS spectrum, $\mathbf{X}_i$, are not dependent on the other MRS spectra, each term in Equation 3 can be minimized independently. Each term in Equation 3 can be rewritten using matrix notation and simplified as shown below.

$$\begin{aligned} RSS_i &= \left(\mathbf{X}_i - \sum_{k=1}^{M} p_{ik}\mathbf{E}_k\right)^T\left(\mathbf{X}_i - \sum_{k=1}^{M} p_{ik}\mathbf{E}_k\right) \\ &= \left(\mathbf{X}_i - \mathbf{E}\mathbf{p}_i\right)^T\left(\mathbf{X}_i - \mathbf{E}\mathbf{p}_i\right) \\ &= \mathbf{X}_i^T\mathbf{X}_i - 2\left(\mathbf{E}\mathbf{p}_i\right)^T\mathbf{X}_i + \left(\mathbf{E}\mathbf{p}_i\right)^T\left(\mathbf{E}\mathbf{p}_i\right) \\ &= \mathbf{X}_i^T\mathbf{X}_i - 2\mathbf{p}_i^T\mathbf{E}^T\mathbf{X}_i + \mathbf{p}_i^T\mathbf{E}^T\mathbf{E}\mathbf{p}_i \end{aligned} \tag{4}$$

where $\mathbf{X}_i$ is the column vector containing the i^{th} MRS spectrum, $\mathbf{p}_i$ is the column vector containing the proportions associated with each endmember and the i^{th} MRS spectrum, and $\mathbf{E}$ is the matrix of endmember spectra where the i^{th} column contains the i^{th} endmember.

2. DATA COLLECTION

A series of *in vitro* experiments were performed to test our algorithms. The experiments were carried out with multipotent astrocytic stem cells (MASCs) which display stem cell characteristics and are 95% astrocytes and a primary neuronal culture. Proton (^{1}H) NMR (MRS) spectra were acquired using a Bruker Avance™-II-600 spectrometer (TopSpin™ software) equipped with a unique 1 mm high-temperature superconducting (HTS) cryoprobe that has between 20 and 25x greater mass sensitivity than a commercial 5-mm probe at the same field strength[15]. Spectra were processed with 2 Hz exponential line broadening before Fourier transformation. Chemical shifts were referenced to lactate methyl doublets, assigned to 1.33 ppm in order to compare spectra with the 2007 *Science* paper by Manganas and others[16]. Spectra were digitally integrated. The cells were not lysed to mimic *in vivo* conditions and emulate what would be seen in a whole brain.

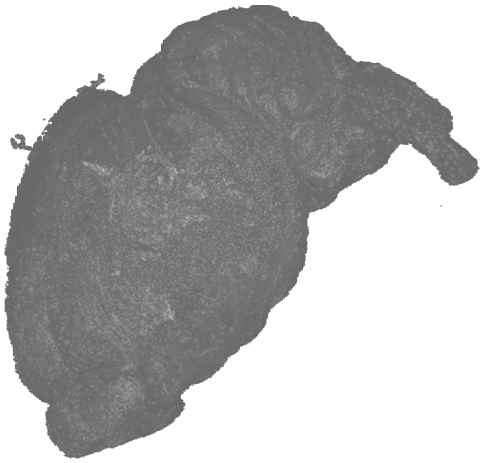

Figure 1: Neuro-imaging Tool Image which allows tracking of stem cells *in vivo* post-transplant

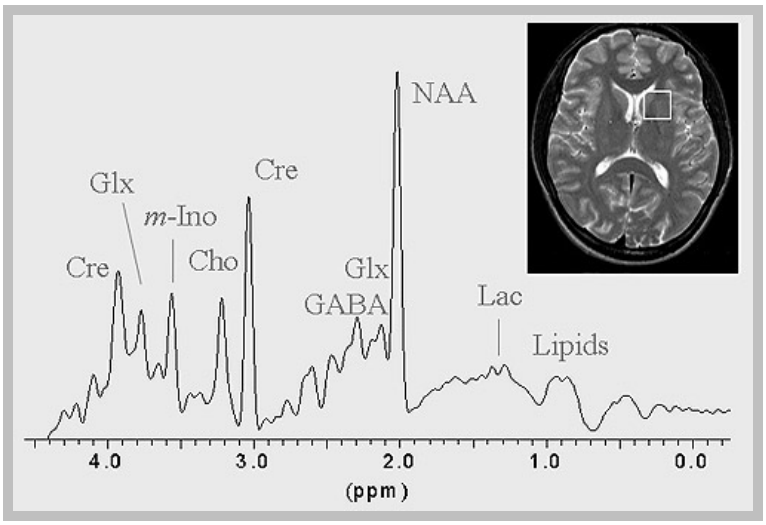

Figure 2: Plot displaying spectrum which can be used to identify metabolites.

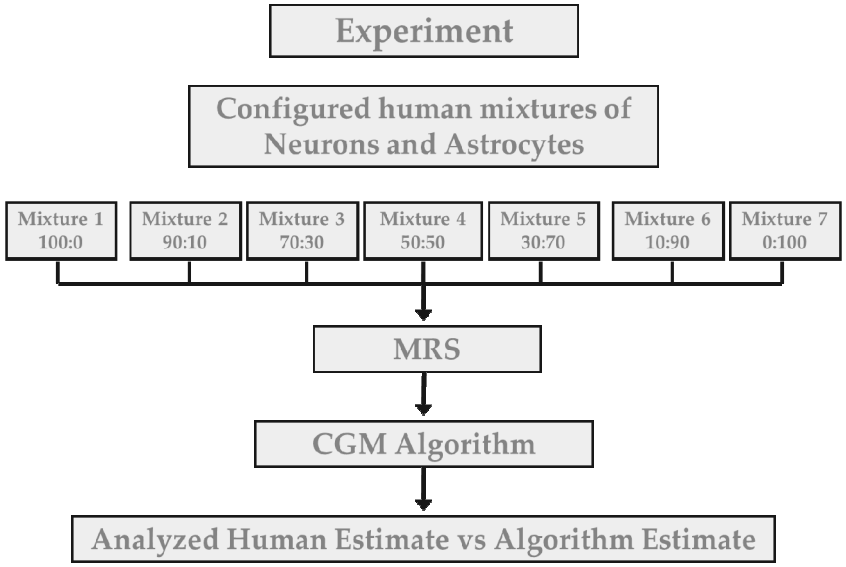

Figure 3: Diagram of Experimental Design

3. RESULTS

In these experiments, mature astrocytes were mixed with mature neurons in a concentration series starting from a pure population of either cell type and then progressing through various concentrations. NMR (MRS) as described above was then performed on each of these samples. Data were collected containing various percentages of neurons and astrocytes. We roughly estimated the percentages of each cell type in the tube based on the number of neurons or astrocytes loaded into each tube. Using spectra from 100% neuron samples and 100% astrocyte samples as endmembers, unmixing yielded the following results based on the NMR data from each of the experimental conditions:

Table 1: Table of results showing the comparison of proportions estimated using the proposed unmixing algorithm and the human expert estimates

Human	Estimate of True Percentage of Neurons	100	90	70	50	30	10	0
Algorithm	Estimate of True Percentage of Neurons	100	94	61	42	32	13	0
Human	Estimate of True Percentage of Astrocytes	0	10	30	50	70	90	100
Algorithm	Estimate of True Percentage of Astrocytes	0	6	39	58	68	87	100

As shown in the table above, the proportion amounts estimated by the spectral unmixing techniques, closely match the estimates made by the human expert for each sample. The overall experimental design is shown in the diagram in Figure 3.

4. CONCLUSIONS

Spectral unmixing of MRS spectra provided accurate estimates of the proportions of cell types and, therefore, shows promise as a tool for tracking stem cells and determining their final phenotypic state. Future work will include construction of larger data sets, mixtures with more cell types, measured both *in vitro* and *in vivo*. Furthermore, spectral unmixing algorithms which incorporate spectral variability into the model will be investigation for this application. Representative distributions for the stem cells will be defined using *in vitro* data samples. In this way, rather than using a single endmember representative for a particular cell type, an endmember distribution can be used which will incorporate any inherent spectral variaibility. After defining the distributions, spectral unmixing to determine the proportions of cell types can be conducted using nonlinear constrained optimization. Also, investigations into methods of incorporating prior knowledge into the ED algorithm's estimation can be conducted. This may be done by incorporating a prior distribution on the distributions for each cell type which will help guide the ED algorithm during estimation of each cell type's distribution. Since the ED algorithm has the capability of estimating unknown endmember distributions, the representative distributions for the stem cells can be held constant while the distributions of the remaining cell types are estimated. This future work may provide a method to account for the portion of cells within a sample that are not stem cells.

REFERENCES

[1] Giffard, R.G., Monyer, H. & Choi, D.W. "Selective vulnerability of cultured cortical glia to injury by extracellular acidosis." Brain Res 530, 138-141 (1990).

[2] MacDonald, H.M., Mulligan, J.C., Allen, A.C. & Taylor, P.M. Neonatal asphyxia. I. "Relationship of obstetric and neonatal complications to neonatal mortality in 38,405 consecutive deliveries." J Pediatr 96, 898-902 (1980).

[3] Finer, N.N., Robertson, C.M., Richards, R.T., Pinnell, L.E. & Peters, K.L. "Hypoxic-ischemic encephalopathy in term neonates: perinatal factors and outcome." J Pediatr 98, 112-117 (1981).

[4] Shankaran, S. "The postnatal management of the asphyxiated term infant." Clin Perinatol 29, 675-692 (2002).

[5] Berger, C. et al. "Effects of hypothermia on excitatory amino acids and metabolism in stroke patients: a microdialysis study." Stroke 33, 519-524 (2002).

[6] Thoresen, M. et al. "Mild hypothermia after severe transient hypoxia-ischemia ameliorates delayed cerebral energy failure in the newborn piglet." Pediatr Res 37, 667-670 (1995).

[7] Bergstedt, K., Hu, B.R. & Wieloch, T. "Postischaemic changes in protein synthesis in the rat brain: effects of hypothermia." Exp Brain Res 95, 91-99 (1993).

[8] Lei, B., Tan, X., Cai, H., Xu, Q. & Guo, Q. "Effect of moderate hypothermia on lipid peroxidation in canine brain tissue after cardiac arrest and resuscitation." Stroke 25, 147-152 (1994).

[9] Battin, M.R., Dezoete, J.A., Gunn, T.R., Gluckman, P.D. & Gunn, A.J. "Neurodevelopmental outcome of infants treated with head cooling and mild hypothermia after perinatal asphyxia." Pediatrics 107, 480-484 (2001).

[10] Gluckman, P.D. et al. "Selective head cooling with mild systemic hypothermia after neonatal encephalopathy: multicentre randomised trial." Lancet 365, 663-670 (2005).

[11] Shankaran, S. et al. "Whole-body hypothermia for neonates with hypoxic-ischemic encephalopathy." N Engl J Med 353, 1574-1584 (2005).

[12] Zheng, T. et al. "Transplantation of multipotent astrocytic stem cells into a rat model of neonatal hypoxic-ischemic encephalopathy." Brain Res 1112, 99-105 (2006).
[13] Englund, U., Bjorklund, A., Wictorin, K., Lindvall, O. & Kokaia, M. "Grafted neural stem cells develop into functional pyramidal neurons and integrate into host cortical circuitry." Proc Natl Acad Sci U S A 99, 17089-17094 (2002).
[14] Vigneron, D.B. et al. "Three-dimensional proton MR spectroscopic imaging of premature and term neonates." AJNR Am J Neuroradiol 22, 1424-1433 (2001).
[15] Brey, W.W. et al. "Design, construction, and validation of a 1-mm triple-resonance high-temperature-superconducting probe for NMR." J Magn Reson 179, 290-293 (2006).
[16] Manganas, L.N. et al. "Magnetic resonance spectroscopy identifies neural progenitor cells in the live human brain." Science 318, 980-985 (2007).
[17] Zare, A. & Gader, P. "PCE: Piece-wise Convex Endmember Detection." IEEE Trans on Geoscience and Remote Sensing (In Review).
[18] Zare, A. & Gader, P. "Sparsity promoting Iterated Constrained Endmember Detection for Hyperspectral Imagery." IEEE Geoscience adn Remote Sensing Letters 4, 446-450 (July 2007).
[19] Nicholson, J.K. & Lindon, J.C. "Systems biology: Metabonomics." Nature 455, 1054-1056 (2008).
[20] Dossey, A.T., Walse, S.S., Rocca, J.R. & Edison, A.S. "Single insect NMR: A new tool to probe chemical biodiversity." ACS Chem Biol 1, 511-514 (2006).
[21] Zhang, F., Dossey, A.T., Zachariah, C., Edison, A.S. & Bruschweiler, R. "Strategy for automated analysis of dynamic metabolic mixtures by NMR. Application to an insect venom." Anal Chem 79, 7748-7752 (2007).
[22] Vannicci, R.C. et al. "Rat model of perinatal hypoxic-ischemic brain damage." J Neurosci Res 55, 158-163. (19
[23] Zheng, T. et al. Transplantation of multipotent astrocytic stem cells into a rat model of neonatal hypoxic-ischemic encephalopathy. Brain Res 1112, 99-105 (2006).
[24] Englund, U., Bjorklund, A., Wictorin, K., Lindvall, O. & Kokaia, M. Grafted neural stem cells develop into functional pyramidal neurons and integrate into host cortical circuitry. Proc Natl Acad Sci U S A 99, 17089-17094 (2002).
[1] Vigneron, D.B. et al. Three-dimensional proton MR spectroscopic imaging of premature and term neonates. AJNR Am J Neuroradiol 22, 1424-1433 (2001).
[2] Brey, W.W. et al. Design, construction, and validation of a 1-mm triple-resonance high-temperature-superconducting probe for NMR. J Magn Reson 179, 290-293 (2006).
[3] Manganas, L.N. et al. Magnetic resonance spectroscopy identifies neural progenitor cells in the live human brain. Science 318, 980-985 (2007).
[4] Zare, A. & Gader, P. PCE: Piece-wise Convex Endmember Detection. IEEE Trans on Geoscience and Remote Sensing (In Review).
[5] Zare, A. & Gader, P. Sparsity promoting Iterated Constrained Endmember Detection for Hyperspectral Imagery. IEEE Geoscience adn Remote Sensing Letters 4, 446-450 (July 2007).
[6] Nicholson, J.K. & Lindon, J.C. Systems biology: Metabonomics. Nature 455, 1054-1056 (2008).
[7] Dossey, A.T., Walse, S.S., Rocca, J.R. & Edison, A.S. Single insect NMR: A new tool to probe chemical biodiversity. ACS Chem Biol 1, 511-514 (2006).
[8] Zhang, F., Dossey, A.T., Zachariah, C., Edison, A.S. & Bruschweiler, R. Strategy for automated analysis of dynamic metabolic mixtures by NMR. Application to an insect venom. Anal Chem 79, 7748-7752 (2007).
[9] Vannicci, R.C. et al. Rat model of perinatal hypoxic-ischemic brain damage. J Neurosci Res 55, 158-163. (1999).
[10] N. Keshava and J. F. Mustard, "Spectral unmixing," *IEEE Signal Processing Magazine*, vol. 19, pp. 44–57, 2002.
[11] J. M. P. Nascimento and J. M. Bioucas-Dias, "Does independent component analysis play a role in unmixing hyperspectral data," *IEEE Transactions on Geoscience and Remote Sensing*, vol. 43, no. 1, pp. 175–187, Jan. 2005.
[12] D. Manolakis, D. Marden, and G. A. Shaw, "Hyperspectral image processing for automatic target detection applications," *Lincoln Laboratory Journal*, vol. 14, no. 1, pp. 79–116, 2003.
[13] M. E. Winter, "Fast autonomous spectral end-member determination in hyperspectral data," in *Proceedings of the Thirteenth International Conference on Applied Geologic Remote Sensing*, Vancouver, B.C., Canada, 1999, pp. 337–344.
[14] J. Boardman, F. Kruse, and R. Green, "Mapping target signatures via partial unmixing of AVIRIS data," in *Summaries of the 5th Annu. JPL Airborne Geoscience Workshop*, R. Green, Ed., vol. 1. Pasadena, CA: JPL Publ., 1995, pp. 23–26.

[15] J. M. P. Nascimento and J. M. B. Dias, "Vertex component analysis: A fast algorithm to unmix hyperspectral data," *IEEE Transactions on Geoscience and Remote Sensing*, vol. 43, no. 4, pp. 898–910, Apr. 2005.
[16] A. Plaza, P. Martinez, R. Perez, and J. Plazas, "Spatial/spectral endmember extraction by multidimensional morphological operators," *IEEE Transactions on Geoscience and Remote Sensing*, vol. 40, no. 9, pp. 2025–2041, Sep. 2002.
[17] D. Lee and H. Seung, "Algorithms for non-negative matrix factorization," in *Advances in Neural Information Processing Systems 13*, 2000, pp. 556–562.
[18] L. Miao and H. Qi, "Endmember extraction from highly mixed data using minimum volume constrained nonnegative matrix factorization," *IEEE Transactions on Geoscience and Remote Sensing*, vol. 45, no. 3, pp. 765–777, Mar. 2007.
[19] P. Pauca, J. Piper, and R. J. Plemmons, "Nonnegative matrix factorization for spectral data analysis," *Linear Algebra Applications*, vol. 416, no. 1, pp. 321–331, Jul. 2005.
[20] S. Jia and Y. Qian, "Constrained nonnegative matrix factorization for hyperspectral unmixing," *IEEE Transactions on Geoscience and Remote Sensing*, vol. 47, no. 1, pp. 161–173, Jan. 2009.
[21] T.-M. Tu, "Unsupervised signature extraction and separation in hyperspectral images: A noise-adjusted fast independent components analysis approach," *Optical Engineering*, vol. 39, no. 4, pp. 897–906, 2000.
[22] J. Wang and C.-I. Chang, "Applications of independent component analysis in endmember extraction and abundance quantification for hyperspectral imagery," *IEEE Transactions on Geoscience and Remote Sensing*, vol. 44, no. 9, pp. 2601–2616, Sep. 2006.
[23] M. D. Craig, "Minimum-volume transforms for remotely sensed data," *IEEE Transactions on Geoscience and Remote Sensing*, vol. 32, no. 3, pp. 542–552, May 1994.
[24] G. X. Ritter, G. Urcid, and M. S. Schmalz, "Autonomous single-pass endmember approximation using lattice auto-associative memories," *Neurocomputing*, vol. 72, pp. 2101–2110, 2009.
[25] J. Nascimento and J. Bioucas-Dias, "Hyperspectral unmixing algorithm via dependent component analysis," in *Proceedings of IEEE: Geoscience and Remote Sensing Symposium*, Barcelona, Spain, July 2007.
[26] N. Dobigeon and J. Tourneret, "Library-based linear unmixing for hyperspectral imagery via reversible jump mcmc sampling," in *Proceedings of the IEEE Aerospace Conference*, Mar. 2009, pp. 1–6.